International Journal of Biochemistry and Cell Biology 110 (2019) 59–69

Contents lists available at ScienceDirect

International Journal of Biochemistry and Cell Biology

journal homepage: www.elsevier.com/locate/biocel

Encapsulated human mesenchymal stem cells (eMSCs) as a novel anti-cancer agent targeting breast cancer stem cells: Development of 3D primed therapeutic MSCs

Saurabh Mandal[a], Frank Arfuso[b,c], Gautam Sethi[d], Arun Dharmarajan[b], Sudha Warrier[a,e,f,*]

[a] Division of Cancer Stem Cells and Cardiovascular Regeneration, School of Regenerative Medicine, Manipal Academy of Higher Education (MAHE), Bangalore, 560 065, India
[b] Stem Cell and Cancer Biology Laboratory, School of Pharmacy and Biomedical Sciences, Curtin Health Innovation Research Institute, Curtin University, Perth, WA, 6102, Australia
[c] School of Human Sciences, The University of Western Australia, Perth, WA, 6009, Australia
[d] Department of Pharmacology, Yong Loo Lin School of Medicine, National University of Singapore, 117 600, Singapore
[e] Curtin Medical School, Curtin University, Perth, Western Australia, 6102, Australia
[f] Cuor Stem Cellutions Pvt Ltd, School of Regenerative Medicine, Manipal Academy of Higher Education (MAHE), Bangalore, 560 065, India

ARTICLE INFO

Keywords:
Encapsulation
Mesenchymal stem cells
Cancer stem cells
sFRP4
3D culture
Sodium alginate
Wnt signaling
eMSCs
EMT

ABSTRACT

Breast cancer is a leading cause of mortality in women across the globe. The major reason for its recurrence and high mortality is due to the presence of a drug refractory and self-renewing population of cells, the cancer stem cells (CSCs). Mesenchymal stem cells (MSCs) have recently emerged as a promising cell-based therapeutic agent for the treatment of different cancer types. However, the anti-tumor effect of MSCs has been indicated to be substantially reduced by their in vivo tumor-trophic migration property and direct cell-to-cell integration with tumor stromal elements. To address this drawback, the present study uses a biomaterial, sodium alginate, for the encapsulation of MSCs from the perinatal tissue, Wharton's jelly (WJMSCs) into microbeads, to study the effect of WJMSCs beads on breast CSCs derived from two breast cancer cell lines, MDA-MB-231 and MCF7. Encapsulation with sodium alginate facilitated the prevention of direct cell-to-cell interaction and these microbeads provided a three-dimensional (3D) microenvironment for the encapsulated WJMSCs (eWJMSCs). Compared to two dimensional (2D) culture, eWJMSC increased proliferation of WJMSCs with an increase in pluripotency genes, epithelial to mesenchymal transition (EMT), immune-modulation, and angiogenesis. Interestingly, the tumor invasion suppressor protein E-cadherin was highly expressed in eWJMSCs as shown by Western blot analysis. In addition, eWJMSCs had an increased secretion of anti-inflammatory cytokines VEGF, TGF-β, TNF-α, IFN-γ, IL-10 and -6, and IL-3β when compared to 2D culture. Treatment of CSCs with eWJMSCs reduced cell viability, inhibited migration, and exerted an anti-angiogenic effect. eWJMSCs treatment of CSCs increased caspase 3/7 activity, nitric oxide production, and reactive oxygen species production, suggesting its anti-tumorigenic activity. Gene expression analysis revealed that CSCs treated with eWJMSCs had a down-regulation of pro-proliferation markers, drug transporters, epithelial-mesenchymal transition-associated markers, and angiogenesis related genes. The mode of anti-proliferative action of WJMSCs beads was possibly through inhibition of the Wnt/β-catenin signaling pathway as indicated by the upregulation of the Wnt antagonists sFRP4 and DKK1. These data suggest that alginate-encapsulated WJMSCs could be an efficient cell contact-free system for developing stem cell-based therapies for CSCs.

1. Introduction

The discovery of mesenchymal stem cells (MSCs) from bone marrow by Friedenstein et al, in 1976 (Friedenstein et al., 1976), as specialized cells capable of self-renewal, proliferation, and multipotent differentiation capability, ignited the new era of tissue engineering and regenerative medicine. From pre-clinical stages to clinical trials, currently MSCs have become a promising therapeutic agent in the treatment of

* Corresponding author at: Division of Cancer Stem Cells and Cardiovascular Regeneration, School of Regenerative Medicine, Manipal Academy of Higher Education (MAHE), Bangalore, 560 065, India.
E-mail address: sudha.warrier@gmail.com (S. Warrier).

https://doi.org/10.1016/j.biocel.2019.02.001
Received 13 October 2018; Received in revised form 28 January 2019; Accepted 1 February 2019
Available online 06 February 2019
1357-2725/

various diseases including cardiovascular and neurological diseases, tissue injury, cancer, and immune disorders (Wang et al., 2004). Interestingly, apart from cell-based tissue replacement therapy, studies suggest that the MSCs or their secretions/secretome may also be promising anti-cancer agents for cancer therapy in mouse models of melanoma (Maestroni et al., 1999), oral cancers (Ji et al., 2016), cholangiosarcoma (Liu et al., 2013), glioma (Nakamura et al., 2004), and bladder cancer (Bitsika et al., 2012). Genetically manipulated MSCs have been used as transport cells, carrying their therapeutic cargo to the site of tumor (Ciavarella et al., 2012; Iskender et al., 2016; Waterman et al., 2012; Bartosh et al., 2010). MSCs, however, have also been shown to have a pro-tumorigenic potential as shown in cervical, ovarian, and pancreatic cancer cells, and the overall effect of MSCs in vivo would depend on the production and interaction of pro- and anti-tumorigenic molecules in the tumor microenvironment (Vizoso et al., 2017).

The closest mimic of the in vivo status of cells in vitro is to grow cells in a three- dimensional (3D) microenvironment simulating the natural environment for cell growth, proliferation, and cell-cell interaction. In the case of MSCs, earlier reports have indicated that 3D culture enhanced the therapeutic action of MSCs and their secretion when compared to standard two-dimensional (2D) monolayer culture. Growth of cells in 3D predominantly tunes the physiological condition of MSCs by regulating the expression of several genes, which increases the level of secreted factors such as growth factors, anti-inflammatory molecules, cytokines, and anti-tumor molecules (Ranganath et al., 2012).

Breast cancer is a leading cause of mortality in women around the globe [GLOBOCAN 2012] (Torre et al., 2015). For the last two decades, it is become very critical to understand the cause of recurrence and high mortality of breast cancer. A notable achievement was the identification of a highly resilient and rare population of cells within the tumor, termed the cancer stem cells (CSCs). CSCs are a small population of cells residing within the tumor bulk and having a similarity to the resident tissue stem cells. After being first identified in 1990 in acute myeloid leukemia and termed “tumor initiating cells” (TICs) (Wang and Dick, 2005), these cells were later identified in breast cancer (Al-Hajj et al., 2003) and subsequently in several cancers including brain (Singh et al., 2003), prostate (Tang et al., 2007), lung (Kim et al., 2005), colorectal (Dalerba et al., 2007) and pancreatic cancers (Li et al., 2007). In breast cancers, CSC have been identified to be positive for CD44 and aldehyde dehydrogenase expressing (ALDH) which correlates with chemoresistance (Ginestier et al., 2007) whereas low or negative for CD24 and lineage negative (16). Conventional anti-cancer treatment only targets the tumor mass, leaving the residing CSC populations untouched (Mukherjee et al., 2014). One of the aberrant signaling pathways implicated in CSC regulation is the Wnt/β-catenin pathway, and abnormal activation of Wnt signaling has been observed in breast CSCs as well as colorectal, hematologic, skin, and lung CSCs (Valkenburg et al., 2011). The Wnt/β-catenin pathway has a definite role in inducing metastasis of breast CSCs (Deshmukh et al., 2017). These observations provide strength to the strategy of targeting Wnt/β-catenin signaling to destroy CSCs.

To investigate the effect of 3D culture of MSCs, in this study we examined the effect of MSCs derived from human Wharton’s jelly (WJMSCs), that were encapsulated in sodium alginate beads, on one of the most prevalent cancers, the breast cancer, and CSCs derived from two breast cancer cell lines, MCF7 and MDA-MB-231. We chose to study the perinatal tissue derived WJMSCs which are now being employed in human clinical trials over MSCs from other sources such as bone marrow or adipose tissue because of the non-invasive harvest from tissue discarded at birth, the relatively high cell yields, phenotypic similarity to that of mesenchymal stromal cells from other tissue sources (Ding et al., 2015) and pro-immunomodulatory properties (Donders et al., 2018). Alginate encapsulation would not only provide a 3D environment for the MSCs, but would also help in avoiding cross-talk between cancer cells and MSCs, a major limitation in the use of MSCs for cancer therapy (Lindoso et al., 2017). We first identified the epithelial-mesenchymal status of encapsulated WJMSCs (eWJMSC) and then evaluated the bonafide immunomodulatory and cytokine secretory properties of WJMSCs grown in a 3D microenvironment by analysing the specific markers to assess a probable antitumorigenic propensity of eWJMSCs. We then studied the effect of eWJMSCs on breast cancer cells and CSCs and examined stemness and tumor suppressive genes, angiogenic and EMT markers and Wnt pathway genes. We also demonstrated functional aspects of apoptosis by caspase, reactive oxygen species, nitric oxide and migration assays and in vivo effect by chick chorioallantoic membrane assay. A clear inhibitory effect of eWJMSCs on CSCs was seen with an indication that the molecular mechanism of inhibition is via the Wnt/β-catenin pathway.

2. Methods

2.1. Cell culture

The enzymatic method of isolation and characterization of WJMSCs is well established and previously reported by our lab (Bhuvanalakshmi et al., 2017a). All the procedures used in the study were approved by the Institutional Ethical Committee (IEC) of Manipal Hospital, Bangalore, India. The WJMSCs were maintained in Dulbecco's Modified Eagle Medium-High Glucose (DMEM-HG) medium (Gibco, Waltham, MA, USA), which was supplemented with fetal bovine serum (FBS) (10%) (Hyclone, USA) and antibiotic solution mix (1%) (Life Technologies) in a CO_2 incubator at 37 °C. Every 3 days, a medium change was given, and WJMSCs of passage 4–5 (P4 to P5) were used for further experiments.

Two human breast cancer cell lines MCF7 and MDA-MB-231 were used in this study and obtained from National Centre for Cell Sciences (NCCS), Pune, India. Both cell lines were maintained in DMEM with 10% FBS and 1% antibiotic solution at 37 °C in 5% CO_2 Incubator. These cells were enriched to breast CSC-like cells and used for further studies. and Cells were cultured in DMEM medium (serum-free) containing 1X B27 (Gibco), an essential supplement added to promote CSC enrichment of CSC in vitro (Chen, 2011), fibroblast growth factor-basic (bFGF) (20 ng/ml) (BioVision, Inc., CA), and epidermal growth factor (EGF) (20 ng/ml) (R&D Systems, Minneapolis, Minnesota). Single cell suspensions of MCF7 and MDA-MB-231 were seeded in ultra-low attachment (Corning Costar) and incubated for 72 h at 37 °C in 5% CO_2 (Bhuvanalakshmi et al., 2017b).

2.2. Encapsulation of WJMSCs

The encapsulation of WJMSCs was performed as reported by Kanafi et al., Li et al. with slight modifications (Kanafi et al., 2014; Li et al., 2011). An alginate solution (2% w/v) was prepared by dissolving 2 g of low viscosity alginic acid sodium salt (Low viscosity 100–300 cP) (Sigma-Aldrich, St. Louis, MO, USA) in 100 ml of deionized water. The alginate solution was mixed by overnight vortexing. The solution was then sterilized using a 0.2 μm syringe filter (Himedia, Mumbai, India). To prepare cell-encapsulated beads, WJMSCs at passage 4 were harvested and a cell density of 5×10^5 was mixed in 1 ml of alginate solution (2% w/v). The alginate solution was transferred to a 5 ml syringe (22 Gauge) and then extruded dropwise into an ice-cold calcium chloride ($CaCl_2$) (Sigma-Aldrich, St. Louis, MO, USA) solution (100 mM). The droplets were left for 10 min in the $CaCl_2$ solution for polymerization. Cell-encapsulated beads were then transferred to 35 mm tissue culture dishes containing 1.5 ml DMEM medium. The WJMSC beads were incubated at 37 °C in 5% CO_2 incubator for 72 h and then used for further experiments.

2.3. Decapsulation

After day three of encapsulation, WJMSC beads were washed with PBS (2 times) and 10 ml of decapsulation solution (EDTA, 50 mM and HEPES, 10 mM in PBS; Sigma-Aldrich, St. Louis, MO, USA) was added and the beads were incubated at 37 °C for 10 min. The cells were recovered by centrifugation at 3000 rpm for 10 min and used for RNA isolation or protein extraction for real-time PCR (qRT-PCR) and Western blotting respectively (Vaithilingam et al., 2011).

2.4. Alamar blue assay

To determine cell proliferation within the alginate beads, the Alamar **blue** assay was performed as previously described by (Schmitt et al., 2015; Nayak et al., 2014). After encapsulating the WJMSCs in alginate beads, cells were incubated for 24 h, considered as day 1. Cell-encapsulated beads and 2D cultured WJMSCs (from day 1 to 5 culture time points) were replenished with fresh medium containing 10% v/v Alamar **blue** reagent (Invitrogen, Carlsbad, CA). After 4 h incubation at 37 °C, absorbance of the media was measured at 570 nm (reduction) and 600 nm (oxidation) using EnSight™ Multimode plate reader (Perkin Elmer) and reduced form of Alamar blue was estimated. Media from cell-free alginate beads was used as the negative control.

2.5. Cell viability assay by calcein-AM staining

The viability of encapsulated cells was assessed by staining with the calcein-AM (Mazzitelli et al., 2010). On day 1, 3, and 5 after encapsulation, 2μM of calcein-AM dye (BD Biosciences, Bedford, MA) was added to the medium and incubated for 30 min at 37 °C. Images were captured using a fluorescence microscope (Olympus IX73). **Green** fluorescence (calcein-AM) was an indicator of live cells.

2.6. Western blotting

The protein expression of Oct-4 and E-cadherin was confirmed by Western blotting (Zhou et al., 2017). After encapsulation for 72 h, beads were decapsulated. The WJMSCs (3D culture) and monolayer grown WJMSCs (2D culture) were lysed in RIPA lysis buffer (50 mM Tris, 150 mM NaCl, 0.1% triton-X 100, 1X proteinase Inhibitor, and 1X phosphatase inhibitor). The cell lysates were centrifuged at 10,000 rpm at 4 °C for 10 min and the supernatant was collected and stored at −20 °C. The lysates were resolved by SDS-PAGE and transferred onto PVDF membranes. After 1 h blocking with Bovine serum albumin (BSA), the membranes were incubated overnight with primary antibodies Oct-4 (1:500, Merck Millipore, #MAB4305), E-cadherin (1:1000, BD Biosciences, #610,181), and β-actin (1:1000, Thermo Fisher, #MA1-140), and horseradish peroxidase-conjugated secondary antibodies (Thermo fisher) were used to bind to the primary antibody and the blot was developed using the TMB Substrate (Sigma-Aldrich, St. Louis, MO, USA); and images were captured using AlphaImager (CA,USA).

2.7. ELISA for determination of cytokine production

WJMSCs cells were encapsulated and cultured for 72 h at CO_2 incubator. The secretome of eWJMSC was collected and centrifuged at 3000 rpm for 5 min. Supernatant was filtered and collected in a tube. The secretome was stored at -80 °C till further use. The level of vascular endothelial growth factor (VEGF), transforming growth factor beta (TGFβ), tumor necrosis factor alpha (TNFα), interferon gamma (IFNγ), interleukins (IL) 10, 6, and 1β in the secretome was quantified using a commercial ELISA kit (R&D Systems, Minneapolis, MN, USA), according to the manufacturer's instructions, and absorbance was measured at 450 nm using an EnSight™ Multimode plate reader (Perkin Elmer). DMEM (serum-free) was used as a control for comparison. Data was normalized using the manufacturer's recommended concentration of standards provided in the kit.

2.8. MTT assay

MCF7 and MDA-MB-231 cells (1×10^4 cells/well) were seeded in low-adherent 96-well plate in a CSC medium consisting of serum-free DMEM supplemented with B27 (1X), bFGF (20 ng/ml) and EGF (20 ng/ml) for 72 h. Cells were treated with day 3 eWJMSC (equal in number) for 48 h. After treatment, 20 μl of MTT (5 mg/PBS) (Himedia, Mumbai, India) was added to the untreated control, empty beads without MSCs and eWJMSC treated cells, and further incubated for 2 h at 37 °C. After incubation, DMSO was added to dissolve the formazan crystals. Absorbance was measured using an EnSight™ Multimode plate reader (Perkin Elmer) at a wavelength at 570 nm. The experiments were performed in triplicate (Warrier et al., 2014).

2.9. RNA isolation and Real time Polymerase chain reaction (qRT-PCR)

Total RNA was isolated from untreated control and treated groups from both MCF7 and MBA-MB-231 CSCs using Trizol reagent (RNAiso Plus, TaKaRa), followed by extraction using chloroform, isopropanol precipitation, and an ethanol wash (70%). 1 μg of RNA sample were converted to cDNA using a PrimeScript™ 1st strand cDNA synthesis kit (TAKARA, Shiga, Japan) as per manufacturer's instructions. The mRNA expression was quantified using SYBR® Premix Ex Taq™ Kit (TAKARA, Shiga, Japan) in a qRT-PCR. cDNA and primers (sequence given in Table 1) were mixed on a MicroAmp Optical tube 8-tube strip (Applied Biosystems). The PCR reaction parameters were 95 °C for 30 s, followed by 40 cycles of 95 °C for 5 s and 60 °C for 31 s. PCR products were verified by melting curves. The endogenous GAPDH expression level was used to normalize the target gene mRNA expression level. Results were calculated based on the $2^{-\Delta\Delta Ct}$ method of a target gene compared to the treated or untreated control samples (Bhuvanalakshmi et al., 2017b).

2.10. Flow cytometry

The effect of WJMSC beads on CD44 expression of enriched CSCs was determined using flow cytometry (Bhuvanalakshmi et al., 2017b). The untreated and treated CSCs were collected, centrifuged at 1500 rpm for 5 min. The cells pellets were washed with PBS (2 times) followed with fixation in 4% paraformaldehyde for 25 min at RT. Fixed cells were washed with PBST twice and kept for blocking for 30 min at RT. After blocking, cells were stained with CD44-FITC (1:200 dilution, BD Biosciences, #560,977) and with appropriate isotype control for 60 min on ice. After staining, cells were washed with PBS and were acquired on BD-FACS calibur flow cytometer and analysis of data was carried out using Cell Quest Pro software.

2.11. Immunocytochemistry

MDA-MB-231 cells (3×10^4 cells/well) were seeded for CSCs, and after 24 h of WJMSC beads treatment, CSCs were fixed with 4% Paraformaldehyde for 20 min at 4 °C followed by permeabilization using Triton X-100 (0.1%) for 15 min at room temperature (RT). CSCs were blocked with 5% BSA prepared in PBS for 30 min at RT. CSCs were incubated with the primary antibody mouse anti-human Ki67 (1:500, BD Biosciences, #550,609) for 2 h at RT and anti-mouse rabbit secondary antibody conjugated to Alexa fluor 488 (1:1000) (Thermo fisher) for 1 h at RT in dark conditions. The nuclei were stained with DAPI (1:10,000). The cells were visualized using an Olympus IX73 fluorescent microscope and photographs were captured using Qimaging-QICAM-fast 1394 (Deshmukh et al., 2017).

Table 1
Primer sequences of target genes.

Gene	Sequence	Tm	Product Size (bp)
Oct-4	F-5'-AGGGCAAGCGATCAAGCA-3' R-5'-GGAAAGGGACCGAGGAGTA-3'	58	166
Sox-2	F-5'-TCAGGAGTTGTCAAGGCAGAG-3' R-5'-TCCGGGCTGTTTTTCTGGTT-3'	60	520
Nanog	F-5'-GCTGGGGAAGGCCTTAATGT-3' R-5'-GCTCCAACCATACTCCACCC-3'	58	277
TNF-alpha	F-5'-TGCTTGTTCCTCAGCCTCTT-3' R-5'-GGTTTGCTACAACATGGGCT-3'	59	199
CXCR4	F-5'-CTGAGAAGCATGACGGACAA-3' R-5'-GACGCCAACATAGACCACCT-3'	59	276
E-cadherin	F-5'-ATTCTGATTCTGCTGCTCTTG-3' R-5'-AGTAGTCATAGTCCTGGTCTT-3'	60	421
N-cadherin	F-5'-CTCCTATGAGTGGAACAGGAACG-3' R-5'-TTGGATCAATGTCATAATCAAGTGCTGTA-3'	63	150
Slug	F-5'-GCTACCCAATGGCCTCTCTC-3' R-5'-CTTCAATGGCATGGGGGTCT-3'	60	170
Snail	F-5'-GAGGCGGTGGCAGACTAG-3' R-5'-GACACATCGGTCAGACCAG-3'	60	178
Twist1	F-5'-CAGCGCACCCAGTCGCTGAA-3' R-5'-CGCCCCACGCCCTGTTTCTT-3'	53	438
HIF-1	F-5'-CTTGGCAACCTTGGATTGGATG-3' R-5'-AATCTCCGTCCCTCAACCTCT-3'	60	190
VEGF	F-5'-CTTGCCTTGCTGCTCTACCT-3' R-5'-GCAGTAGCTGCGCTGATAGA-3'	60	123
CD44	F-5'-CATCTACCCCAGCAACCCTA-3' R-5'-GGTTGTGTTTGCTCCACCTT-3'	56	397
CD24	F-5'-AACTAATGCCACCACCAAGG-3' R-5'-CCTGTTTTTCCTTGCCACAT-3'	55	188
ALDH1	F-5'-AGGGCCAGTGTTGTATAGCC-3' R-5'-TCCACATTCCAGTTTGGCCC-3'	60	218
Cyclin D1	F-5'-CGTCCATGCGGAAGATC-3' R-5'-CAGAGGGCAACGAAGGT-3'	61	406
Ki67	F-5'-GAGAATCTGTGAATCTGGGTAA-3' R-5'-CAGGCTTGCTGAGGGAAT-3'	62	279
NF-κB	F-5'- ATGGAGAGTTGCTACAACCCA-3' R-5'-CTGTTCCACGATCACCAGGTA-3'	60	135
XIAP	F- 5'-GGGGTTCAGTTTCAAGGACA-3' R-5'-CGCCTTAGCTGCTCTTCAGT-3'	56	183
ABCC2	F-5'-AGAGCTGGCCCTTGTACTCA-3' R-5'-TGCGTTTCAAACTTGCTCAC-3'	60	492
TIE-2	F-5'-CCCCTATGGGTGTTCCTGT-3' R-5'-GCTTACAATCTGGCCCGTAA-3'	60	89
Angiopoietin1	F-5'- TCGAATTGAAATGTGTGAGGCA-3' R-5'- GGAAGTGGAGAGGGACTGAA-3'	58	228
sFRP4	F-5'-CGATCGGTGCAAGTGTAAA-3' R-5'-GACTTGAGTTCGAGGGATGG-3'	60	180
DKK1	F-5'-TCCGAGGAGAAATTGAGGAA-3' R-5'-CCTGAGGCACAGTCTGATGA-3'	59	157
GSK-3β	F-5'-ACTCCAGTGGCGAGAAGAAA-3' R-5'-TTGAGGACAGCAGTGTCAGG-3'	55	241
AXIN2	F-5'-CTGGCTATGTCTTTGCACCA-3' R-5'-AGGAGGGATTCCATCTACGC-3'	58	113
β-catenin	F-5'-CGTCCACAACACTCTGGCTA-3' R-5'-GCCAGCACTTCACTGCAATA-3'	55	159

2.12. Caspase assay

After treatment of MDA-MB-231 CSCs (1×10^4 cells/well) with and without eWJMSC, caspase 3/7 activity, a mediator of apoptosis, was measured using CellEvent™ caspase-3/7 **green** detection reagent (Thermo fisher) in serum free DMEM medium for 30 min at 37 °C in the dark. The fluorescence intensity was measured using an EnSight™ Multimode plate reader (Perkin Elmer) at an excitation wavelength of 503 nm and an emission wavelength of 535 nm. Stained cells were also observed under fluorescence microscopy (Oroz-Parra et al., 2016).

2.13. Intracellular reactive oxygen species (ROS) assay

To measure the onset of apoptosis by the release of ROS, an indicator of apoptosis (Bhuvanalakshmi et al., 2017b), intracellular ROS level was measured using a fluorometric intracellular ROS kit (Sigma-Aldrich, St. Louis, MO, USA) as per the manufacturer's instructions. Briefly, 1×10^4 cells per well were seeded for CSC formation in a 96-well plate. MDA-MB-231 CSCs were treated with WJMSC beads for 48 h. After treatment, untreated and treated cells were incubated with ROS reagent for 30 min at 37 °C in the dark, and fluorescence intensity was measured using an EnSight™ Multimode plate reader (Perkin Elmer) at 650 nm (excitation) and 675 nm (emission).

2.14. Griess assay

Nitric oxide (NO) production, which has been reported to initiate apoptosis (Umansky et al., 2000), was determined using the Griess. A cell density of 2×10^4 MDA-MB-231 CSCs per well in a 96 well plate were prepared. The CSCs were treated with eWJMSC for 48 h. After incubation, an equal volume of Griess reagent (Sigma-Aldrich, St. Louis, MO, USA) was added to each well of control and treated cells. The cells were incubated for 30 min at 37°C in a CO_2 incubator. The absorbance was measured at 550 nm on an EnSight™ Multimode plate reader (Perkin Elmer). The percentage of NO production of untreated and eWJMSCs treated was calculated as previously described (Bhuvanalakshmi et al., 2017a).

2.15. Transwell migration assay

The cell migration assay to determine inhibition of migration was performed by transwell migration assay according to protocol previously reported (Bhuvanalakshmi et al., 2017b). Briefly, untreated and eWJMSC treated MDA-MB-231 CSCs were seeded equally (2×10^4) onto the transwell upper compartment and the lower chamber were filled with CSC medium. After 48 h of incubation at 37°C in a 5% CO_2 incubator, the migrated CSCs on the under-surface of the membrane were stained with 0.5% Crystal Violet for 5 min. The cells were visualized under an inverted microscope as described previously (Mukherjee et al., 2014).

2.16. In vivo chick chorioallantoic membrane (CAM) Assay

To analyze the in vivo anti-angiogenic effectiveness of WJMSC beads, a CAM assay was performed by the protocol previously reported (Teruszkin Balassiano et al., 2001). Embryonated eggs of days 4 or 5 were obtained from Veterinary College, Bangalore, India. All the procedures used in the study were approved by the Institutional Ethical Committee (IEC). MDA-MB-231 CSCs (as untreated controls) were injected in the air sac region using a syringe needle according to previously reported protocols (Bhuvanalakshmi et al., 2017b). In the treatment group, CSCs were injected and then WJMSC beads were added in the air sac region. Eggs were incubated at 37°C for 48 h. Then the shell was removed carefully to expose the membrane and observed for changes in the vascularization pattern. Each treatment condition was performed in triplicate.

2.17. Statistical analysis

All data were represented as mean and SD obtained from the experiments. All the experiments were performed in triplicate. Statistical significance was assessed by the Student's *t*-test (unpaired). $p < 0.05$ was considered significant for all statistical analyses.

3. Results

3.1. Characterization of WJMSCs cultured in sodium alginate beads

After isolation of WJMSCs, cells of passage 4 (P4) were used for encapsulation in sodium alginate beads. Photomicrographs showed

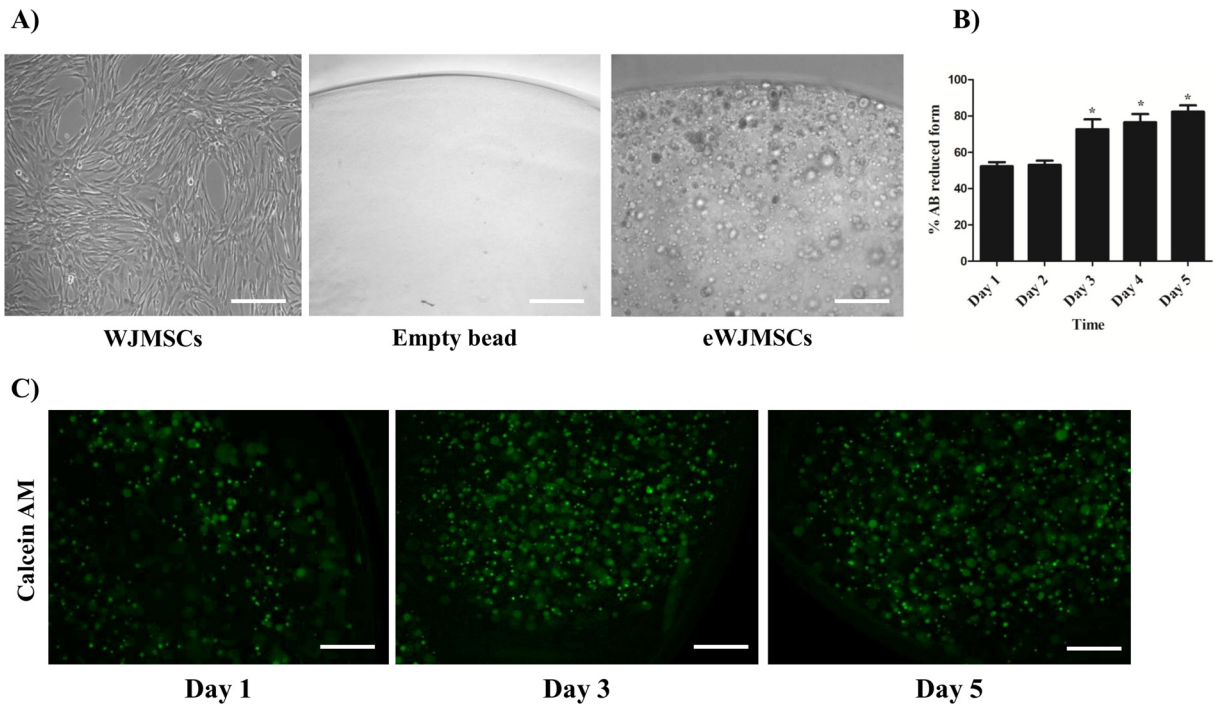

Fig. 1. Growth analysis of WJMSCs in sodium alginate beads. (A) Photomicrographs of WJMSCs in monolayer culture (left panel) and in sodium alginate beads without and with WJMSCs (middle and right panel respectively). (B) Proliferation of eWJMSCs determined by Alamar Blue assay (% AB reduced form) from day 1 to 5. Results are the mean ± SD, *$p < 0.05$. (C) Fluorescent microscopic images of eWJMSCs after staining with calcein-AM at day 1, 3, and 5 indicating cell proliferation (scale bar = 100 μm, n = 3).

cells were rounded in appearance after encapsulation within beads (Fig. 1A). To determine cell proliferation, an Alamar Blue assay was performed wherein the reduced form of Alamar Blue, resorufin, is measured, which is proportional to the number of living cells thereby indicating increased proliferation. Increase in Alamar Blue (reduced form) confirmed that the WJMSCs proliferated after encapsulation within the sodium alginate beads at different time periods (Fig. 1B). Day 1 and 2 showed a similar result, which was 52.29% and 53.04% respectively. On day 3, 4 and 5 there was a spurt in proliferation indicated by increase to 73%, 77% and 83% respectively, indicating active proliferation of WJMSCs within the alginate capsule. Similarly, calcein-AM staining was carried out (Fig. 1C) and increased green fluorescence observed on day 1, 3, and 5 demonstrates the proliferation of WJMSCs.

3.2. 3D culture of eWJMSCs regulates pluripotency, epithelial-mesenchymal transition (EMT), immunomodulation, and pro-angiogenic gene expression

The expression of genes regulating pluripotency, EMT, immunomodulation and angiogenesis was significantly higher in eWJMSCs as compared to the 2D monolayer culture (Fig. 2A). The expression of pluripotent genes Oct-4, Sox-2, and Nanog in eWJMSCs was 64.5%, 61.5%, and 61.2% respectively, in comparison to 2D cultured WJMSCs, which was 43.2%, 45.8%, and 49.9% respectively. The immunomodulatory genes TNF-alpha and CXCR4 expression were analyzed, which was 59.7% and 66.4% in eWJMSCs and 40.8% and 54.6% in 2D monolayer cultured WJMSCs respectively. The expression of EMT markers E-cadherin, N-Cadherin, Slug, Snail, and Twist1 was 55.3%, 72.3%, 75%, 74.9%, and 73% respectively, in 3D, while in the 2D monolayer was 23.2%, 43.4%, 60.2%, 64.9%, and 55.8%, respectively. A significant increase was observed in expression of pro-angiogenic genes hypoxia-inducible factor-1 (HIF-1) and VEGF, 80.4% and 74% respectively, in 3D cells, whereas it was 27.7% and 55.3% respectively, in 2D cultured cells.

3.3. Presence of secretory cytokines in eWJMSC secretome

MSCs secrete well known signaling factors that have paracrine effects. An ELISA was carried out to quantify the factors secreted by monolayer culture of WJMSCs and eWJMSCs (Fig. 2B). We found a total of seven paracrine signaling factors such as VEGF, TGF-β, TNF-α, IFN-γ, IL-10, IL-6, and IL-1β, which were present at a higher level in eWJMSC medium compared to the control WJMSCs conditioned medium.

3.4. 3D encapsulation regulates Oct-4 and E-cadherin protein expression in WJMSCs

Following gene expression, we investigated the protein expression level of the epithelial marker E-cadherin and pluripotent marker Oct-4 in eWJMSCs. Results demonstrated a higher protein level of Oct4 in eWJMSCs when compared with 2D cultured WJMSCs (Fig. 2C), suggesting that a 3D microenvironment could enhance pluripotency of MSCs.

3.5. Enrichment and characterization of breast CSCs

We enriched the CSCs in MCF7, MDA-MB-231 cell lines by culture them in serum free, CSC specific medium and obtained CSCs spheres (Fig. 3A). The cultured CSCs were characterized for the CSC specific markers CD44, CD24, and ALDH by real-time quantitative PCR (Fig. 3B) wherein CD44 and ALDH expressions were upregulated whereas CD24 was downregulated. The qPCR of MCF7 and MDA-MB CSCs results confirmed that CD44 (34.5% in MCF, 36.8% in MDA) and ALDH (12% in MCF, 10.5% in MDA) had increased expressions whereas CD24 expression (15% in MCF7, 10.5% in MDA-MB) was decreased when compared to non CSC monolayer cells.

3.6. eWJMSCs reduces viability of breast CSCs

We evaluated the effect of eWJMSCs in the MCF7 and MDA-MB-231

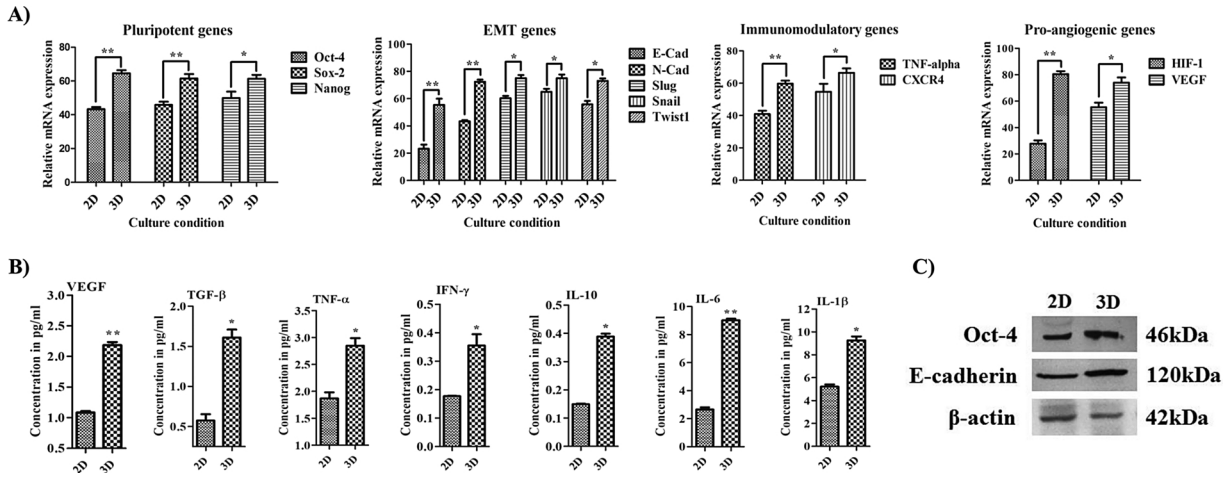

Fig. 2. 3D culture upregulated EMT, immunomodulatory genes and enhanced the level of secretory cytokines of eWJMSCs when compared to 2D culture (A) Gene expression analysis by qRT-PCR of pluripotent markers Oct4, Sox2, and Nanog; EMT genes E-cadherin, N-cadherin, Slug, Snail, and Twist1; immuno-modulatory markers TNFα and CXCR4; pro-angiogenic genes HIF-1α and VEGF. (B) Western blot of Oct-4 and E-cadherin of 2D and 3D cultured WJMSCs. Data represent an average of three independent experiments. **(C)** ELISA analysis of secretory cytokines VEGF, TGFβ, TNFα, IFNγ, IL10, IL6, and IL1β in medium derived from 2D and 3D WJMSCs cultures. Results are the mean ± SD of three independent experiments performed in triplicates, *p < 0.05, **p < 0.01.

CSCs using an MTT assay. As shown in Fig. 3D, eWJMSC treatment for 48 h caused disruption of spheres and about 57% and 49% decrease in viability of MCF7 CSCs and MDA-MB-231 CSCs respectively. However, treatment with empty beads had no effect on proliferation (Fig. 3C1, C2). Furthermore, eWJMSCs treatment reduced the CD44 expression significantly compared to control CSCs shown by flow cytometry (Fig. 3E). Based on these data, sodium alginate beads prepared with 2×10^5 cells per ml and 48 h incubation were used for further downstream experiments.

3.7. eWJMSCs suppresses proliferation, induces apoptosis, and down-regulates drug transporters in MCF7 and MDA-MB-231 CSCs

We analyzed the mRNA expression by real-time PCR of proliferation associated markers, Cyclin D1 and Ki67 after eWJMSCs treatment, and observed a decrease of 31.3% and 38.47% respectively in MCF7 CSCs (Fig. 4A); in MDA-MB-231 CSCs decrease was 53.5% and 34.8% respectively (Fig. 4E). Next, we examined the expression of apoptotic genes nuclear factor kappa-light-chain-enhancer of activated B cells (NF-κB) and X-linked inhibitor of apoptosis protein (XIAP) in breast CSCs. The results showed that eWJMSCs caused a reduction of 15.7% in NF-κB and 28.5% in XIAP expression in MCF7 CSCs; while in MDA-MB-231 CSCs, there was a reduction of 29% in NF-kB and 38.3% in XIAP gene inhibition in comparison to untreated CSCs. eWJMSC treatment down-regulated the expression of the drug transporter gene ABCC2 in MCF7- and MDA-MB-231- CSCs by 22.9% and 17.9% respectively.

3.8. eWJMSCs down-regulate EMT promoting genes

The real-time PCR was used to determine the gene expression of

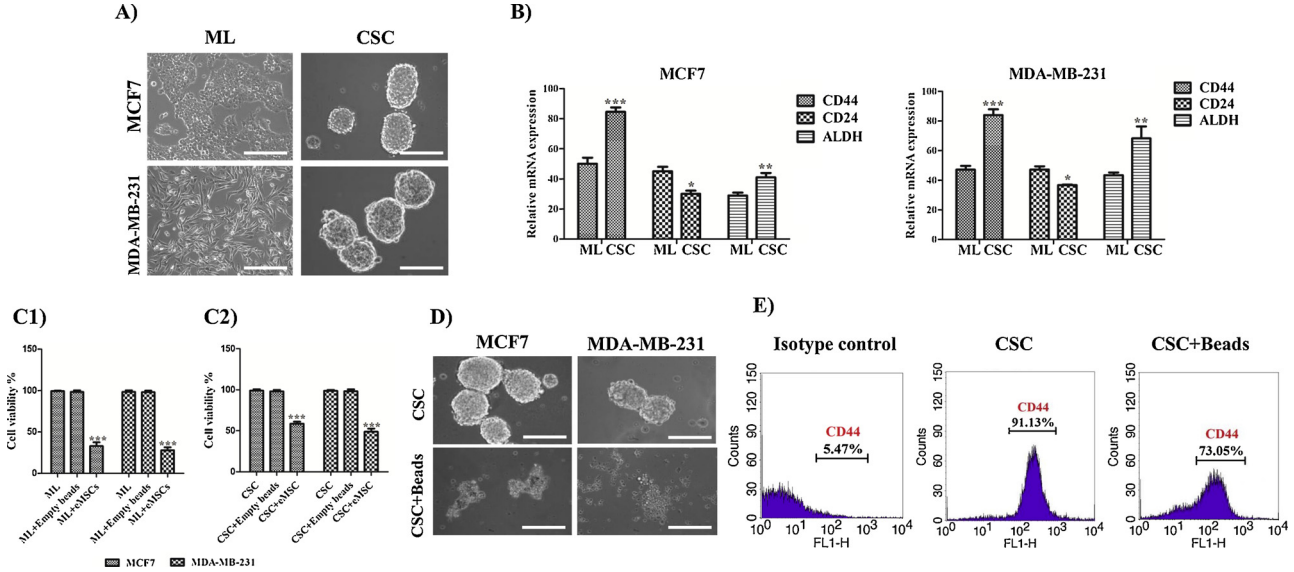

Fig. 3. Characterisation of breast CSC markers in sphere cultures and the effect of eWJMSCs on CSC viability. (A) Photomicrographs of monolayer culture (left panel) and CSC sphere (right panel) culture of MCF7 and MDA-MB-231 cell lines. **(B)** qRT-PCR analysis indicating signature expression of CSC markers CD44, CD24 and ALDH in CSC culture compared to monolayer culture indicating enrichment of CSCs. Data represent an average of three independent experiments, mean ± SD, *p < 0.05, **p < 0.01 ***p < 0.001. **(C)** Representative photomicrographs of untreated CSCs and eWJMSC-treated CSCs derived from MCF-7 and MDA-MB-231. (D) Cell viability by MTT assay. **(E)** Flow cytometry analysis to estimate the CD44 expression in CSCs control and eWJMSC-treated CSCs. Data represent an average of three independent experiments, mean ± SD, ***p < 0.001 (Scale bar = 50 μm).

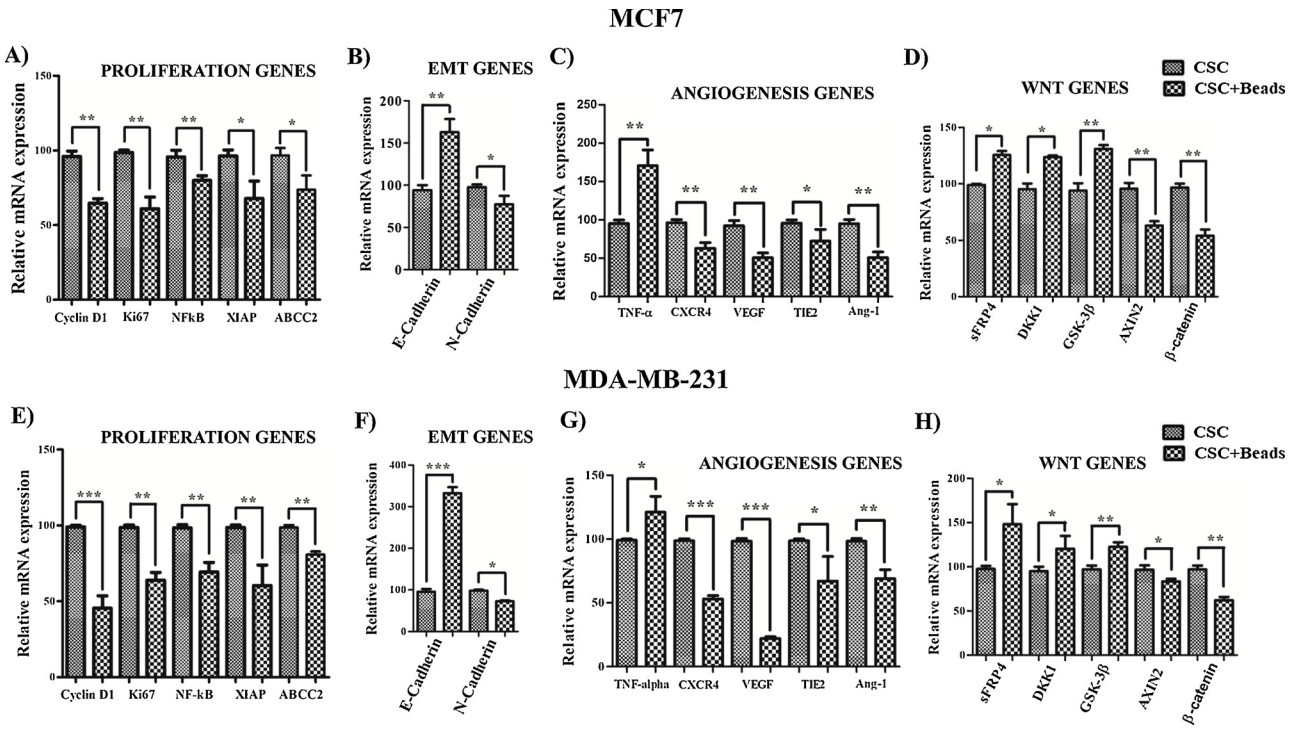

Fig. 4. eWJMSC treatment inhibited tumor-associated genes in CSCs. qRT-PCR gene expression of CSCs and eWJMSC-treated CSCs derived from MCF-7 (A–D) and MDA-MB-231 cells (E–H) respectively, of pro-proliferation markers, apoptotic genes, and drug transporter (A, E), EMT associated markers (B, F), angiogenesis related genes (C, G), and Wnt modulators (D, H). Results are the mean ± SD, *p < 0.05, **p < 0.01 ***p < 0.001.

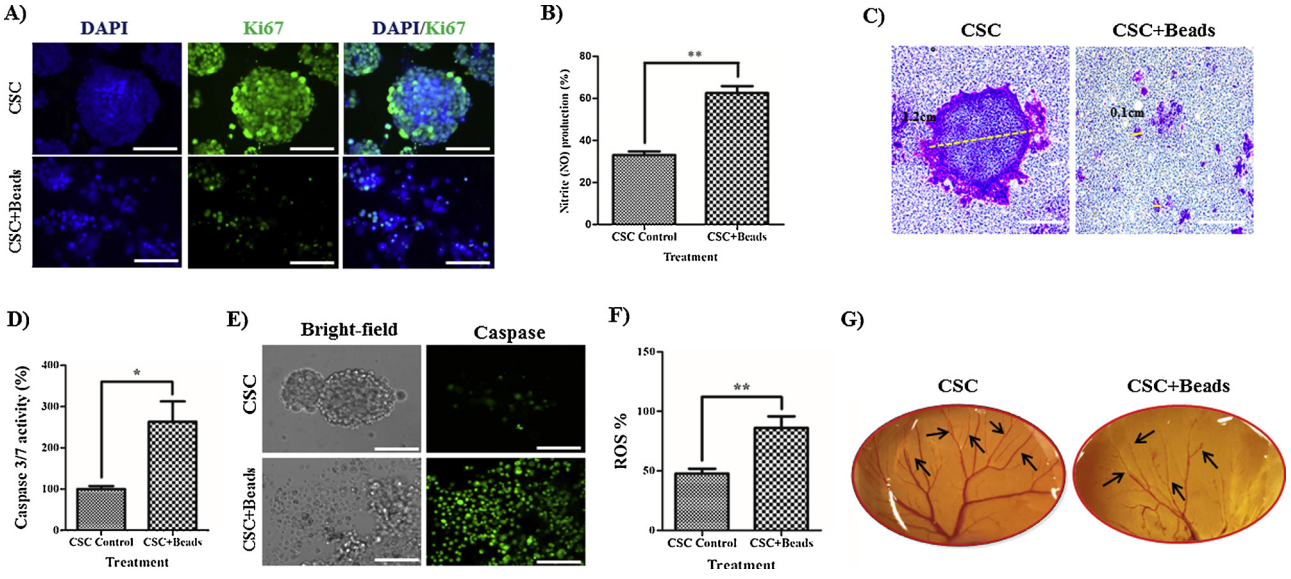

Fig. 5. eWJMSCs treatment affects CSC functionality. (A) Fluorescence microscopy of Ki67 staining indicated eWJMSC treatment (beads) disrupted CSC spheres and reduced the expression of Ki67. (B) Greiss assay indicating NO production. (C) Transwell migration assay and crystal violet staining indicating eWJMSC (beads) treatment inhibited the migration ability of CSCs. (D) Caspase-3/7 activity determined by caspase assay (left panel) and fluorescence microscopy (right panel) indicated increased caspase activity in eWJMSC (beads) treated CSCs. (E) ROS release was determined using a fluorometric intracellular ROS assay (F). The angiogenic property was determined in vivo by CAM assay in the untreated and eWJMSC (beads) treated MDA-MB-231 CSCs. Results are the mean ± SD, n = 5, *p < 0.05 and **p < 0.01 (Scale bar = 50 μM). Arrows indicate healthy (untreated) and the disrupted (beads treated) vasculature. Images are representative of experiments performed in triplicates.

EMT markers in CSCs after eWJMSC treatment. The results indicated that the E-cadherin expression was significantly up-regulated while there was down-regulation of N-cadherin expression in CSCs from both MCF7 (Fig. 4B) and MDA-MB-231 (Fig. 4F) CSCs. In comparison to the untreated CSC controls, E-cadherin expressed 68.8% higher and 231.2% higher in eWJMSC treated MCF7- and MDA-MB-231- CSCs respectively. N-cadherin was inhibited by 20.4% in MCF7 CSCs and 12% in MDA-MB-231 CSCs after eWJMSC treatment.

3.9. Effect of eWJMSCs on immuno-modulatory and angiogenesis markers

We next aimed to determine the changes of immuno-modulatory and angiogenesis-associated gene expression. Treatment of CSCs eWJMSCs not only resulted in a significant increase in expression of

TNF-α but also a decrease in proangiogenic markers in both MCF7 and MDA-MB CSCs. In addition, CXCR4, TIE2, and Angiopoietin-1 expression showed a significant decrease in both MCF7- and MDA-MB-231-CSCs after treatment with eWJMSCs (Fig. 4C,G).

3.10. eWJMSCs treatment targets Wnt signaling in breast CSCs

We next investigated the gene expression of the Wnt pathway modulators secreted frizzled-related protein 4 (sFRP4), Dickkopf 1 (DKK1), glycogen synthase kinase-3 beta (GSK-3β), AXIN2 and β-catenin. In MCF7 CSCs, in response to eWJMSC treatment, the transcript level of sFRP4, DKK1, and GSK-3β increased by 13.6%, 22%, and 26.4% respectively while the AXIN2 and β-catenin level decreased by 32.6% and 42.6% respectively (Fig. 4D). Results were similar in MDA-MB-231 CSCs, (Fig. 4H) in which an increase of 50.3% of sFRP4, 25.3% of DKK1, and 25.6% of GSK-3β was observed, whereas a 13.3% and 34.6% decrease was observed in AXIN2 and β-catenin expression respectively in MDA-MB-231 CSCs after eWJMSC treatment.

3.11. Reduction of proliferation marker protein ki67 in CSCs after eWJMSC treatment

We confirmed a reduction in a key proliferation marker protein ki67 by immunocytochemistry (Fig. 5A), where MDA-MB-231 CSCs were labelled with the proliferation marker ki67. The eWJMSC treatment showed disruption of spheres and a reduction in ki67 expression when compared to the untreated CSCs.

3.12. eWJMSCs induces nitric oxide (NO) production

Further we looked into the release of apoptotic-inducing factors such as nitric oxide (NO) (Vahora et al., 2016). The NO production in untreated MDA-MB-231 CSCs and eWJMSCs treated CSCs were assessed using the Griess Assay and showed a marked increase in the treatment group (Fig. 5B). The NO level was also increased in the eWJMSC treated CSCs (66.5%) as compared to untreated MDA-MB-231 CSCs (33%).

3.13. eWJMSCs inhibits the migration of CSCs

To assess the ability of eWJMSCs to inhibit the migration of breast CSCs, which indicates the migratory and metastatic potential, we carried out a migration assay using transwell chambers. After the incubation of MDA-MB-231 CSCs with eWJMSCs, migrated cells were stained with crystal violet dye. We observed a 85% of reduction in migration in eWJMSC treated CSCs compared to untreated CSCs (Fig. 5C). These significant results indicate that eWJMSCs reduced the migratory ability of CSCs.

3.14. eWJMSCs treatment activates caspase 3/7 activity in CSCs

The quantitation of caspase-3 and -7 activity in the MDA-MB-231 CSCs after treatment with the eWJMSCs was performed. The results obtained from the fluorescence intensity at excitation/emission wavelength ~ 503/530 nm (Fig. 5D) as well as fluorescence microscopy images (Fig. 5E) indicated 1.5 fold high caspase3/7 activity in comparison to the untreated CSC control.

3.15. eWJMSCs increases the intracellular ROS level

Release of ROS, an indicator of initiation of the apoptotic pathway (Redza-Dutordoir and Averill-Bates, 2016), was measured to further substantiate apoptosis. The intracellular ROS level in MDA-MB-231 CSCs with eWJMSCs treatment was drastically higher (86%) than that of the untreated CSCs (47.7%) (Fig. 5F).

3.16. eWJMSCs exert anti-angiogenesis effects against MDA-MB-231 CSCs

The CAM assay outcome showed potential anti-angiogenic activity of the eWJMSCs treated MDA-MB 231 CSCs, which caused a reduction in vascularization compared to the untreated CSCs control (Fig. 5G).

4. Discussion

In this study, we have explored the anti-cancer activity of WJMSCs encapsulated in sodium alginate beads against robust breast CSCs. It has been proven that 3D culture of MSCs enhances their paracrine action, cell survival, and differentiation capacity when compared to conventional 2D culture, since it provides more physiological environment for the cells (Cesarz and Tamama, 2016; Xie et al., 2016). This is in line with a previous report from Penolazzi et al. for encapsulation of WJMSCs using sodium alginate (Penolazzi et al., 2010).

The eWJMSCs in this study showed rapid increase in proliferation and enhanced viability as measured by Alamar blue and calcein-AM respectively. Poor survival of MSCs is one of the drawbacks of transplantation (Li et al., 2016). Hence, it is anticipated that 3D microstructure and mild hypoxia within the alginate beads facilitated in proper cell growth and viability of eWJMSCs, which ultimately contribute to the higher therapeutic efficiency of MSCs in vivo.

The properties of MSCs can be influenced by several mechanical parameters such as adhesion, geometry, and elasticity (Fletcher and Mullins, 2010; McBeath et al., 2004). It has been found that culturing cells in 2D fails to maintain expression of pluripotent genes Sox-2, Oct-4, and Nanog, which results in a low self-renewal ability (Zhou et al., 2017; Frith et al., 2010). This is consistent with our results showing a lower expression of pluripotent genes in monolayer compared to eWJMSCs, wherein the expression level of Oct-4, Sox-2, and Nanog in eWJMSCs was significantly increased and is thus evidently essential in maintaining the stem cells' pluripotency. Along with enhancement in pluripotent gene expression, cell-to-cell interaction is also crucial for MSCs to maintain their stem cell fate. EMT genes play an important role in the establishment of cell-to-cell interaction and exchange of signals between cells, which could also affect the production of paracrine molecules (Georgopoulos et al., 2010). An earlier study suggested that E-cadherin mediates cell-to-cell interaction in spheroid cultures of MSCs (Lee et al., 2012). In our study we observed upregulation of the epithelial marker E-cadherin indicating mesenchymal-to-epithelial transition (MET) but contrastingly other markers such as N-cadherin, slug, snail, and twist were also overexpressed indicative of EMT phenotype. This observation points to a hybrid E and M population within the alginate microbead similar to previous reports using alginate based 3D matrices (Bidarra et al., 2016). An increased protein expression of stemness marker, Oct-4 in eWJMSCs suggested that 3D culture could maintain the stemness traits of MSCs.

Lack of homing capacity and angiogenesis of MSCs are some limiting factors in transplantation therapy. Several studies reported that cytokines and growth factors are important MSC homing mediators, and are involved in their angiogenesis and migration, as well as exerting anti-tumour activities (Wang et al., 2004; Cesarz and Tamama, 2016; Potapova et al., 2007; Kwon et al., 2013; Yang et al., 2015). The elevated transcript levels of CXCR4, TNF-α and VEGF in eWJMSCs may be attributed to the stimulation of a paracrine mechanism to facilitate migration and angiogenesis. In addition, upregulation of the master hypoxia gene HIF-1 reflects the hypoxic conditions that prevail within beads and that enhanced the eWJMSCs' hallmark features. On examination of the level of some cytokines we found that compared to the monolayer culture, eWJMSC secretome contains a higher concentration of VEGF, TGF-β, TNF-α, IFN-γ, IL-10, IL-6, and IL-1β, all of which have a potential role in MSC homing, angiogenesis, proliferation, and in the treatment of multiple disorders (Bartosh et al., 2010; Madrigal et al., 2014).

After establishing the potential anti-tumor activity of eWJMSCs, we

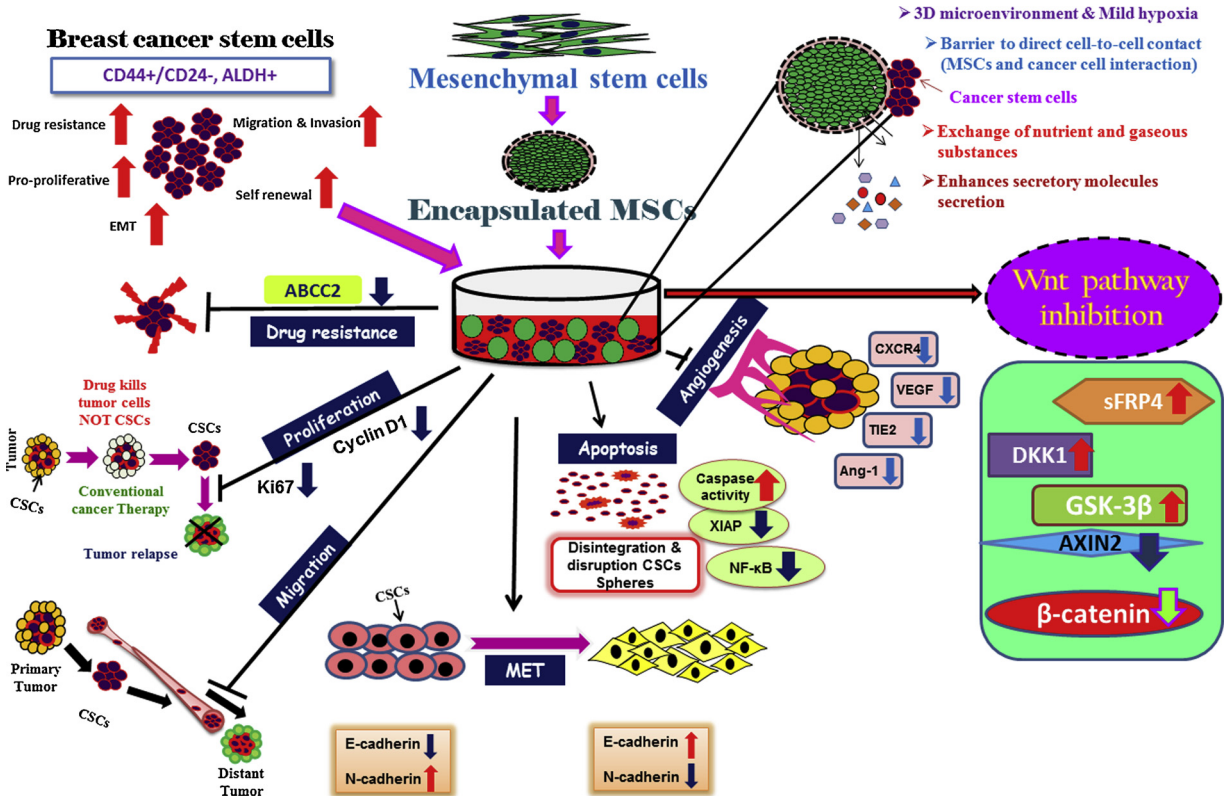

Scheme 1. 3D primed therapeutic MSCs to target cancer stem cells. Alginate encapsulated MSCs fosters exchange of molecules, induces hypoxia, prevents cell-cell contact and inhibits CSC-specific properties (drug resistance, proliferation, migration and angiogenesis) and facilitates apoptosis by the promoting inhibitors of the Wnt pathway such as sFRP4, DKK1 and GSK3β.

probed the effect on breast CSCs that were characterized and enriched from breast cancer cell lines, MCF7 and MDA-MB-231. The decrease in proliferation and induction of apoptosis as noted in the reduction of pro-proliferative genes ki67, cyclin D1, NF-kB and inhibitor of apoptosis protein XIAP, established the inhibitory effect of eWJMSCs on the resilient CSC population. Furthermore there was a reduction in chemoresistance inducers such as ABCC2 marker. Additionally, ROS which was over produced in eWJMSC-treated CSCs also probably mediated damage to DNA via disrupting plasma membrane integrity and destabilizing the actin cytoskeleton (Simon et al., 2000; Gourlay and Ayscough, 2005). Another mechanism of abrogation of CSCs by eWJMSC could also be by NO production which increased after treatment by the cytotoxic, anti-metastatic, and pro-apoptotic activity of NO that has been reported to inhibit the proliferation of human breast cancer cells (Reveneau et al., 1999; Onier et al., 1999). In our study, we noticed a high amount of NO production in treated CSCs, which may be linked to iNOS gene upregulation.

In breast CSCs, EMT is associated with anti-cancer drug resistance, post-treatment relapse, tumor invasion, and metastasis (Luo et al., 2015). Loss of E-cadherin and subsequent higher expression of N-cadherin lead to cell-polarity disruption, which is the main cause of EMT (Kotiyal and Bhattacharya, 2014; Wang et al., 2015). We noted that eWJMSC treatment in MCF7 and MDA-MB-231 CSCs reversed the expression EMT promoting genes E-cadherin and N-cadherin, which could result in lowering of tumor migration, invasion, and resistance. This was further corroborated by retardation in CSC migration after eWJMSC treatment in a transwell migration assay. Overall, the restored EMT suppressor E-cadherin level, lower β-catenin expression, and activation of GSK-3β in eWJMSC- treated CSCs could be linked to the suppression of CSC migration (Mukherjee et al., 2014; Goncalves Ndo et al., 2016; Mao et al., 2012).

TNF-α is a cytokine involved in diverse cellular processes such as inflammation (Bradley, 2008), cell survival and death (Zelova and Hosek, 2013), differentiation (Gupta, 2002; Azuma et al., 2000), angiogenesis (Kwon et al., 2013), and migration (Prisco et al., 2016). It has also been well characterized as an anti-tumorigenic factor (Pfeffer, 2003) and inducing apoptotic cell death in various cancers (van Horssen et al., 2006). We observed high expression of the TNF-α gene, which could be the reason for the elevated pro-apoptotic response observed in our study. In addition, we also observed downregulation in cytokines and growth factors related to angiogenesis. VEGF a key regulator of tumor angiogenesis, and also induces the production of the cytokine CXCR4 to promote cancer migration (Shibuya, 2011). Analysis of breast cancer cell lines as well as clinical samples suggests there is elevated expression of these growth factors (Carmeliet, 2005). Another well-characterized endothelial cell-specific receptor tyrosine kinase TIE2 complex with its ligand Angiopoietin-1 (Ang-1) facilitating tumor angiogenesis angiogenesis (Xu et al., 2015; Chatterjee et al., 2014; Stratmann et al., 2001). We demonstrated a downregulation of all the proangiogenic mediators, CXCR4, VEGF, TIE2, and Ang-1 in breast CSCs after treatment with eWJMSCs. Our in vivo CAM assay results also demonstrate physical inhibition of angiogenesis of CSCs indicating the anti-angiogenic effect of eWJMSCs.

Evidence suggests that the Wnt/β-catenin pathway, which is one of the conserved signaling systems in cancer, not only regulates the development and progression of CSCs but also promotes their stemness, metastasis, proliferation, and survival (de Sousa and Vermeulen, 2016). An increased level of β-catenin, a notable finding in breast CSCs, is found to be associated with CSC self-renewal and migration, and is linked to transcribing the ABCB1/MDR-1 gene (Yamada et al., 2003). The endogenous Wnt antagonists sFRPs and DKK1 compete with Wnt protein and prevent its binding to a frizzled receptor, which inhibits the Wnt system. In breast CSCs, these antagonists are remarkably downregulated (Bhuvanalakshmi et al., 2017b). The sFRP family of 1–5, of which sFRP4 has prominent anti-angiogenic and pro-apoptotic properties (Deshmukh et al., 2017; Bhuvanalakshmi et al., 2017b; Warrier

et al., 2014; Saran et al., 2017). We have previously reported that an exogenous addition of sFRP4 (Warrier et al., 2014; Bhuvanalakshmi et al., 2015) and overexpression of sFRP4 (Bhuvanalakshmi et al., 2019) retards the CSCs' properties and chemo-sensitizes cells towards chemotherapeutic drugs. In addition we showed that specifically in breast CSC, a natural compound diosgenin exerted an anti-CSC action by targeting the active Wnt pathway and inducing expression of antgonists such as sFRP4 and DKK1 (Bhuvanalakshmi et al., 2017b). Axin2, a key component of the β-catenin destruction complex, plays a role as a negative regulator of the Wnt pathway in normal cells, but can act as a tumor promoter by facilitating EMT (Wu et al., 2012). Our results document an increase of sFRP4, DKK1, and GSK-3β expression in eWJMSC treatment of CSCs, which was associated with the down-regulation of β-catenin and axin2 suggesting that axin2 would have a tumor promoting role.

In summary, we can conclude that 3D encapsulation augmented the stem cell properties and increased the paracrine secretions of WJMSCs. eWJMSCs exhibit anti-cancer activity against breast CSCs, down-regulate several cancer-associated genes, and inhibit Wnt pathways via triggering Wnt antagonism. eWJMSCs not only inhibit migration and angiogenesis of breast CSCs but also target their functionality by caspase activation and increase ROS and NO production (Scheme 1). Development of eWJMSCs as a promising cell based therapy could help to target the core refractory cancer stem cells and reduce the burden and relapse of breast cancer.

Conflict of interest statement

Authors declare no conflict of interest.

Acknowledgments

This work was supported partly by funding to SW from the Department of Biotechnology, India (No. BT/PR9235/MED/31/258/2014), Indian Council of Medical Research, India (No. 90/24/2012-BMS) and Intramural Research Funding to the School of Regenerative Medicine (SORM) from Manipal Academy of Higher Education (MAHE), Manipal, India. SM is thankful for the support (TMA Pai PhD Scholarship) from MAHE.

References

Al-Hajj, M., Wicha, M.S., Benito-Hernandez, A., Morrison, S.J., Clarke, M.F., 2003. Prospective identification of tumorigenic breast cancer cells. Proc. Natl. Acad. Sci. U. S. A. 100 (7), 3983–3988.
Azuma, Y., Kaji, K., Katogi, R., Takeshita, S., Kudo, A., 2000. Tumor necrosis factor-alpha induces differentiation of and bone resorption by osteoclasts. J. Biol. Chem. 275 (7), 4858–4864.
Bartosh, T.J., Ylostalo, J.H., Mohammadipoor, A., Bazhanov, N., Coble, K., et al., 2010. Aggregation of human mesenchymal stromal cells (MSCs) into 3D spheroids enhances their antiinflammatory properties. Proc. Natl. Acad. Sci. U. S. A. 107 (31), 13724–13729.
Bhuvanalakshmi, G., Arfuso, F., Millward, M., Dharmarajan, A., Warrier, S., 2015. Secreted frizzled-related protein 4 inhibits glioma stem-like cells by reversing epithelial to mesenchymal transition, inducing apoptosis and decreasing cancer stem cell properties. PLoS One 10 (6), e0127517.
Bhuvanalakshmi, G., Arfuso, F., Kumar, A.P., Dharmarajan, A., Warrier, S., 2017a. Epigenetic reprogramming converts human Wharton's jelly mesenchymal stem cells into functional cardiomyocytes by differential regulation of Wnt mediators. Stem Cell Res. Ther. 8 (1), 185.
Bhuvanalakshmi, G., Basappa, Rangappa K.S., Dharmarajan, A., Sethi, G., et al., 2017b. Breast Cancer Stem-Like cells are inhibited by Diosgenin, a steroidal saponin, by the attenuation of the wnt beta-catenin signaling via the Wnt antagonist secreted frizzled related Protein-4. Front. Pharmacol. 8, 124.
Bhuvanalakshmi, G., Gamit, N., Patil, M., Arfuso, F., Sethi, G., et al., 2019. Stemness, pluripotentiality, and Wnt antagonism: sFRP4, a Wnt antagonist mediates pluripotency and stemness in glioblastoma. Cancers 11 (1), 25.
Bidarra, S., Oliveira, P., Rocha, S., Saraiva, D., Oliveira, C., et al., 2016. A 3D in vitro model to explore the inter-conversion between epithelial and mesenchymal states during EMT and its reversion. Sci. Rep. 6, 27072.
Bitsika, V., Roubelakis, M.G., Zagoura, D., Trohatou, O., Makridakis, M., et al., 2012. Human amniotic fluid-derived mesenchymal stem cells as therapeutic vehicles: a novel approach for the treatment of bladder cancer. Stem Cells Dev. 21 (7), 1097–1111.
Bradley, J.R., 2008. TNF-mediated inflammatory disease. J. Pathol. 214 (2), 149–160.
Carmeliet, P., 2005. VEGF as a key mediator of angiogenesis in cancer. Oncology 69 (Suppl. 3), 4–10.
Cesarz, Z., Tamama, K., 2016. Spheroid culture of mesenchymal stem cells. Stem Cells Int., 9176357 2016.
Chatterjee, S., Behnam Azad, B., Nimmagadda, S., 2014. The intricate role of CXCR4 in cancer. Adv. Cancer Res. 124, 31–82.
Chen, H., 2011. The effect of B27 supplement on promoting in vitro propagation of Her2/neu- transformed mammary tumorspheres. J. Biotech Res. 3, 7.
Ciavarella, S., Grisendi, G., Dominici, M., Tucci, M., Brunetti, O., et al., 2012. In vitro anti-activity of TRAIL-expressing adipose-derived mesenchymal stem cells. Br. J. Haematol. 157 (5), 586–598.
Dalerba, P., Dylla, S.J., Park, I.K., Liu, R., Wang, X., et al., 2007. Phenotypic characterization of human colorectal cancer stem cells. Proc. Natl. Acad. Sci. U. S. A. 104 (24), 10158–10163.
de Sousa, E.M.F., Vermeulen, L., 2016. Wnt signaling in Cancer stem cell biology. Cancers (Basel) 8 (7).
Deshmukh, A., Kumar, S., Arfuso, F., Newsholme, P., Dharmarajan, A., 2017. Secreted Frizzled- related protein 4 (sFRP4) chemo-sensitizes cancer stem cells derived from human breast, prostate, and ovary tumor cell lines. Sci. Rep. 7 (1), 2256.
Ding, D.C., Chang, Y.H., Shyu, W.C., Lin, S.Z., 2015. Human umbilical cord mesenchymal stem cells: a new era for stem cell therapy. Cell Transplant. 24 (3), 339–347.
Donders, R., Bogie, J.F.J., Ravanidis, S., Gervois, P., Vanheusden, M., et al., 2018. Human Wharton's jelly-derived stem cells display a distinct immunomodulatory and pro-regenerative transcriptional signature compared to bone marrow-derived stem cells. Stem Cells Dev. 27 (2), 65–84.
Fletcher, D.A., Mullins, R.D., 2010. Cell mechanics and the cytoskeleton. Nature 463 (7280), 485–492.
Friedenstein, A.J., Gorskaja, J.F., Kulagina, N.N., 1976. Fibroblast precursors in normal and irradiated mouse hematopoietic organs. Exp. Hematol. 4 (5), 267–274.
Frith, J.E., Thomson, B., Genever, P.G., 2010. Dynamic three-dimensional culture methods enhance mesenchymal stem cell properties and increase therapeutic potential. Tissue Eng. Part C Methods 16 (4), 735–749.
Georgopoulos, N.T., Kirkwood, L.A., Walker, D.C., Southgate, J., 2010. Differential regulation of growth-promoting signalling pathways by E-cadherin. PLoS One 5 (10), e13621.
Ginestier, C., Hur, M.H., Charafe-Jauffret, E., Monville, F., Dutcher, J., et al., 2007. ALDH1 is a marker of normal and malignant human mammary stem cells and a predictor of poor clinical outcome. Cell Stem Cell 1 (5), 555–567.
Goncalves Ndo, N., Colombo, J., Lopes, J.R., Gelaleti, G.B., Moschetta, M.G., et al., 2016. Effect of melatonin in epithelial mesenchymal transition markers and invasive properties of breast Cancer stem cells of canine and human cell lines. PLoS One 11 (3), e0150407.
Gourlay, C.W., Ayscough, K.R., 2005. The actin cytoskeleton: a key regulator of apoptosis and ageing? Nat. Rev. Mol. Cell Biol. 6 (7), 583–589.
Gupta, S., 2002. A decision between life and death during TNF-alpha-induced signaling. J. Clin. Immunol. 22 (4), 185–194.
Iskender, B., Izgi, K., Sakalar, C., Canatan, H., 2016. Priming hMSCs with a putative anti-cancer compound, myrtucommulone-a: a way to harness hMSC cytokine expression via modulating PI3K/Akt pathway? Tumour Biol. 37 (2), 1967–1981.
Ji, X., Zhang, Z., Han, Y., Song, J., Xu, X., et al., 2016. Mesenchymal stem cells derived from normal gingival tissue inhibit the proliferation of oral cancer cells in vitro and in vivo. Int. J. Oncol. 49 (5), 2011–2022.
Kanafi, M.M., Ramesh, A., Gupta, P.K., Bhonde, R.R., 2014. Dental pulp stem cells immobilized in alginate microspheres for applications in bone tissue engineering. Int. Endod. J. 47 (7), 687–697.
Kim, C.F., Jackson, E.L., Woolfenden, A.E., Lawrence, S., Babar, I., et al., 2005. Identification of bronchioalveolar stem cells in normal lung and lung cancer. Cell 121 (6), 823–835.
Kotiyal, S., Bhattacharya, S., 2014. Breast cancer stem cells, EMT and therapeutic targets. Biochem. Biophys. Res. Commun. 453 (1), 112–116.
Kwon, Y.W., Heo, S.C., Jeong, G.O., Yoon, J.W., Mo, W.M., et al., 2013. Tumor necrosis factor-alpha-activated mesenchymal stem cells promote endothelial progenitor cell homing and angiogenesis. Biochim. Biophys. Acta 1832 (12), 2136–2144.
Lee, E.J., Park, S.J., Kang, S.K., Kim, G.H., Kang, H.J., et al., 2012. Spherical bullet formation via E-cadherin promotes therapeutic potency of mesenchymal stem cells derived from human umbilical cord blood for myocardial infarction. Mol. Ther. 20 (7), 1424–1433.
Li, C., Heidt, D.G., Dalerba, P., Burant, C.F., Zhang, L., et al., 2007. Identification of pancreatic cancer stem cells. Cancer Res. 67 (3), 1030–1037.
Li, L., Davidovich, A.E., Schloss, J.M., Chippada, U., Schloss, R.R., et al., 2011. Neural lineage differentiation of embryonic stem cells within alginate microbeads. Biomaterials 32 (20), 4489–4497.
Li, L., Chen, X., Wang, W.E., Zeng, C., 2016. How to improve the survival of transplanted mesenchymal stem cell in ischemic heart? Stem Cells Int., 9682757 2016.
Lindoso, R.S., Collino, F., Vieyra, A., 2017. Extracellular vesicles as regulators of tumor fate: crosstalk among cancer stem cells, tumor cells and mesenchymal stem cells. Stem Cell Investig. 4, 75.
Liu, J., Han, G., Liu, H., Qin, C., 2013. Suppression of cholangiocarcinoma cell growth by human umbilical cord mesenchymal stem cells: a possible role of Wnt and Akt signaling. PLoS One 8 (4), e62844.
Luo, M., Brooks, M., Wicha, M.S., 2015. Epithelial-mesenchymal plasticity of breast cancer stem cells: implications for metastasis and therapeutic resistance. Curr. Pharm. Des. 21 (10), 1301–1310.
Madrigal, M., Rao, K.S., Riordan, N.H., 2014. A review of therapeutic effects of

mesenchymal stem cell secretions and induction of secretory modification by different culture methods. J. Transl. Med. 12, 260.
Maestroni, G.J., Hertens, E., Galli, P., 1999. Factor(s) from nonmacrophage bone marrow stromal cells inhibit Lewis lung carcinoma and B16 melanoma growth in mice. Cell. Mol. Life Sci. 55 (4), 663–667.
Mao, L., Dauchy, R.T., Blask, D.E., Slakey, L.M., Xiang, S., et al., 2012. Circadian gating of epithelial-to-mesenchymal transition in breast cancer cells via melatonin-regulation of GSK3beta. Mol. Endocrinol. 26 (11), 1808–1820.
Mazzitelli, S., Capretto, L., Zhang, X.L., Penolazzi, L., Lambertini, E., et al., 2010. Process optimization for the production of alginate microparticles containing wjmscs by a design of experiments (doe) approach. J. Control. Release 148 (1), e76–77.
McBeath, R., Pirone, D.M., Nelson, C.M., Bhadriraju, K., Chen, C.S., 2004. Cell shape, cytoskeletal tension, and RhoA regulate stem cell lineage commitment. Dev. Cell 6 (4), 483–495.
Mukherjee, S., Mazumdar, M., Chakraborty, S., Manna, A., Saha, S., et al., 2014. Curcumin inhibits breast cancer stem cell migration by amplifying the E-cadherin/beta-catenin negative feedback loop. Stem Cell Res. Ther. 5 (5), 116.
Nakamura, K., Ito, Y., Kawano, Y., Kurozumi, K., Kobune, M., et al., 2004. Antitumor effect of genetically engineered mesenchymal stem cells in a rat glioma model. Gene Ther. 11 (14), 1155–1164.
Nayak, S., Dey, S., Kundu, S.C., 2014. Silk sericin-alginate-chitosan microcapsules: hepatocytes encapsulation for enhanced cellular functions. Int. J. Biol. Macromol. 65, 258–266.
Onier, N., Hilpert, S., Reveneau, S., Arnould, L., Saint-Giorgio, V., et al., 1999. Expression of inducible nitric oxide synthase in tumors in relation with their regression induced by lipid A in rats. Int. J. Cancer 81 (5), 755–760.
Oroz-Parra, I., Navarro, M., Cervantes-Luevano, K.E., Alvarez-Delgado, C., Salvesen, G., et al., 2016. Apoptosis activation in human lung Cancer cell lines by a novel synthetic peptide derived from Conus californicus venom. Toxins (Basel) 8 (2), 38.
Penolazzi, L., Tavanti, E., Vecchiatini, R., Lambertini, E., Vesce, F., et al., 2010. Encapsulation of mesenchymal stem cells from Wharton's jelly in alginate microbeads. Tissue Eng. Part C Methods 16 (1), 141–155.
Pfeffer, K., 2003. Biological functions of tumor necrosis factor cytokines and their receptors. Cytokine Growth Factor Rev. 14 (3-4), 185–191.
Potapova, I.A., Gaudette, G.R., Brink, P.R., Robinson, R.B., Rosen, M.R., et al., 2007. Mesenchymal stem cells support migration, extracellular matrix invasion, proliferation, and survival of endothelial cells in vitro. Stem Cells 25 (7), 1761–1768.
Prisco, A.R., Hoffmann, B.R., Kaczorowski, C.C., McDermott-Roe, C., Stodola, T.J., et al., 2016. Tumor necrosis factor alpha regulates endothelial progenitor cell migration via CADM1 and NF-kB. Stem Cells 34 (7), 1922–1933.
Ranganath, S.H., Levy, O., Inamdar, M.S., Karp, J.M., 2012. Harnessing the mesenchymal stem cell secretome for the treatment of cardiovascular disease. Cell Stem Cell 10 (3), 244–258.
Redza-Dutordoir, M., Averill-Bates, D.A., 2016. Activation of apoptosis signalling pathways by reactive oxygen species. Biochim. Biophys. Acta 1863 (12), 2977–2992.
Reveneau, S., Arnould, L., Jolimoy, G., Hilpert, S., Lejeune, P., et al., 1999. Nitric oxide synthase in human breast cancer is associated with tumor grade, proliferation rate, and expression of progesterone receptors. Lab. Invest. 79 (10), 1215–1225.
Saran, U., Mani, K.P., Balaguru, U.M., Swaminathan, A., Nagarajan, S., et al., 2017. sFRP4 signalling of apoptosis and angiostasis uses nitric oxide-cGMP-permeability axis of endothelium. Nitric Oxide 66, 30–42.
Schmitt, A., Rodel, P., Anamur, C., Seeliger, C., Imhoff, A.B., et al., 2015. Calcium alginate gels as stem cell matrix-making paracrine stem cell activity available for enhanced healing after surgery. PLoS One 10 (3), e0118937.
Shibuya, M., 2011. Vascular endothelial growth factor (VEGF) and its receptor (VEGFR) signaling in angiogenesis: a crucial target for Anti- and pro-angiogenic therapies. Genes Cancer 2 (12), 1097–1105.
Simon, H.U., Haj-Yehia, A., Levi-Schaffer, F., 2000. Role of reactive oxygen species (ROS) in apoptosis induction. Apoptosis 5 (5), 415–418.
Singh, S.K., Clarke, I.D., Terasaki, M., Bonn, V.E., Hawkins, C., et al., 2003. Identification of a cancer stem cell in human brain tumors. Cancer Res. 63 (18), 5821–5828.
Stratmann, A., Acker, T., Burger, A.M., Amann, K., Risau, W., et al., 2001. Differential inhibition of tumor angiogenesis by tie2 and vascular endothelial growth factor receptor-2 dominant-negative receptor mutants. Int. J. Cancer 91 (3), 273–282.
Tang, D.G., Patrawala, L., Calhoun, T., Bhatia, B., Choy, G., et al., 2007. Prostate cancer stem/progenitor cells: identification, characterization, and implications. Mol. Carcinog. 46 (1), 1–14.
Teruszkin Balassiano, I., Alves De Paulo, S., Henriques Silva, N., Curie Cabral, M., da Gloria da Costa Carvalho, M., 2001. Metastatic potential of MDA435 and Hep2 cell lines in chorioallantoic membrane (CAM) model. Oncol. Rep. 8 (2), 431–433.
Torre, L.A., Bray, F., Siegel, R.L., Ferlay, J., Lortet-Tieulent, J., et al., 2015. Global cancer statistics, 2012. CA Cancer J. Clin. 65 (2), 87–108.
Umansky, V., Ushmorov, A., Ratter, F., Chlichlia, K., Bucur, M., et al., 2000. Nitric oxide-mediated apoptosis in human breast cancer cells requires changes in mitochondrial functions and is independent of CD95 (APO-1/Fas). Int. J. Oncol. 16 (1), 109–117.
Vahora, H., Khan, M.A., Alalami, U., Hussain, A., 2016. The potential role of nitric oxide in halting cancer progression through chemoprevention. J. Cancer Prev. 21 (1), 1.
Vaithilingam, V., Quayum, N., Joglekar, M.V., Jensen, J., Hardikar, A.A., et al., 2011. Effect of alginate encapsulation on the cellular transcriptome of human islets. Biomaterials 32 (33), 8416–8425.
Valkenburg, K.C., Graveel, C.R., Zylstra-Diegel, C.R., Zhong, Z., Williams, B.O., 2011. Wnt/beta-catenin signaling in normal and Cancer stem cells. Cancers (Basel) 3 (2), 2050–2079.
van Horssen, R., Ten Hagen, T.L., Eggermont, A.M., 2006. TNF-alpha in cancer treatment: molecular insights, antitumor effects, and clinical utility. Oncologist 11 (4), 397–408.
Vizoso, F.J., Eiro, N., Cid, S., Schneider, J., Perez-Fernandez, R., 2017. Mesenchymal stem cell secretome: toward cell-free therapeutic strategies in regenerative medicine. Int. J. Mol. Sci. 18 (9).
Wang, J.C., Dick, J.E., 2005. Cancer stem cells: lessons from leukemia. Trends Cell Biol. 15 (9), 494–501.
Wang, H.S., Hung, S.C., Peng, S.T., Huang, C.C., Wei, H.M., et al., 2004. Mesenchymal stem cells in the Wharton's jelly of the human umbilical cord. Stem Cells 22 (7), 1330–1337.
Wang, S.S., Jiang, J., Liang, X.H., Tang, Y.L., 2015. Links between cancer stem cells and epithelial-mesenchymal transition. Onco. Ther. 8, 2973–2980.
Warrier, S., Bhuvanalakshmi, G., Arfuso, F., Rajan, G., Millward, M., et al., 2014. Cancer stem -like cells from head and neck cancers are chemosensitized by the Wnt antagonist, sFRP4, by inducing apoptosis, decreasing stemness, drug resistance and epithelial to mesenchymal transition. Cancer Gene Ther. 21 (9), 381–388.
Waterman, R.S., Henkle, S.L., Betancourt, A.M., 2012. Mesenchymal stem cell 1 (MSC1)-based therapy attenuates tumor growth whereas MSC2-treatment promotes tumor growth and metastasis. PLoS One 7 (9), e45590.
Wu, Z.Q., Brabletz, T., Fearon, E., Willis, A.L., Hu, C.Y., et al., 2012. Canonical Wnt suppressor, Axin2, promotes colon carcinoma oncogenic activity. Proc. Natl. Acad. Sci. U. S. A. 109 (28), 11312–11317.
Xie, L., Mao, M., Zhou, L., Jiang, B., 2016. Spheroid mesenchymal stem cells and mesenchymal stem cell-derived microvesicles: two potential therapeutic strategies. Stem Cells Dev. 25 (3), 203–213.
Xu, C., Zhao, H., Chen, H., Yao, Q., 2015. CXCR4 in breast cancer: oncogenic role and therapeutic targeting. Drug Des. Dev. Ther. 9, 4953–4964.
Yamada, T., Mori, Y., Hayashi, R., Takada, M., Ino, Y., et al., 2003. Suppression of intestinal polyposis in Mdr1-deficient ApcMin/+ mice. Cancer Res. 63 (5), 895–901.
Yang, J.X., Zhang, N., Wang, H.W., Gao, P., Yang, Q.P., et al., 2015. CXCR4 receptor overexpression in mesenchymal stem cells facilitates treatment of acute lung injury in rats. J. Biol. Chem. 290 (4), 1994–2006.
Zelova, H., Hosek, J., 2013. TNF-alpha signalling and inflammation: interactions between old acquaintances. Inflamm. Res. 62 (7), 641–651.
Zhou, Y., Chen, H., Li, H., Wu, Y., 2017. 3D culture increases pluripotent gene expression in mesenchymal stem cells through relaxation of cytoskeleton tension. J. Cell. Mol. Med. 21 (6), 1073–1084.